DE GRUYTER High Temperature Materials and Processes 2023; 42: 20220276

Research Article

Shixian Zhang, Kai Hu, Xiaoping Zhao, Jinglong Liang, and Yungang Li*

Study on diffusion kinetics of chromium and nickel electrochemical co-deposition in a NaCl–KCl–NaF–Cr_2O_3–NiO molten salt

https://doi.org/10.1515/htmp-2022-0276
received November 16, 2022; accepted May 02, 2023

Abstract: The process of preparing surface composite by molten salt co-deposition is the result of the mass transfer of active particles in molten salt, electrochemical reduction, and solid diffusion. In this study, we prepared Cr–Ni alloy/low-carbon steel surface composites in NaCl, KCl, NaF, Cr_2O_3, and NiO melt salt system successfully, and analyzed the entire diffusion dynamics process, aiming to find out the limiting links and provide ideas for further improving the preparation efficiency. The results show that chromium and nickel ions are simultaneously reduced on the cathode surface through two and one steps, respectively. And an alloy layer with Fe content of 64.52 wt%, Ni content of 28.96 wt%, and Cr content of 6.52 wt% is formed on the surface of low-carbon steel substrate. The average diffusion coefficients of chromium and nickel atoms in the surface composites are 1.16×10^{-14} and 1.44×10^{-14} $m^2 \cdot s^{-1}$. The mass transfer process in molten salt is the limiting link in the whole preparation process.

Keywords: electrochemical co-deposition, diffusion kinetics, Cr–Ni alloy/low-carbon steel surface composite, diffusion mechanism, diffusion coefficients, melt salt

1 Introduction

Electrochemical deposition in molten salt is one of the most important methods to prepare surface composites. This method can not only carry out the reduction of oxides and the purification of rare metals but can also prepare metallurgical bonded surface gradient composites in one step, which are widely used in metallurgical production, energy, environmental protection, material preparation and other industrial technology fields. Sun et al. [1] deposited high-purity tungsten with good adhesion on the graphite cathode. Dubrovskiy et al. [2] electrochemically synthesized Mo_2C coatings with different structures on molybdenum substrate. Yasuda et al. [3] studied the effect of temperature and current density on the electrodeposition of Si films in KF–KCl–K_2SiF_6 molten salt system, and experimentally obtained the diffusion coefficient of Si^{4+} ions. Zhang [4] studied the co-deposition behavior of Ce(III) and Mg(II) on tungsten electrodes in $CaCl_2$–NaCl melt, and calculated the diffusion coefficient of ions. Huang et al. [5] studied the electrochemical reduction process of Y(III) and the cathodic behavior of Y_2O_3 in YF_3–LiF molten salt system, and calculated the diffusion coefficient of Y(III). Wang et al. [6] prepared silicide coatings containing $MoSi_2$ and Si–$MoSi_2$ by electrodeposition on molybdenum substrate, and discussed the relevant deposition mechanism. Huang et al. [7–10], respectively, deposited Ir coatings on graphite, Re, and Mo cathodes. Kuznetsov [11] electrodeposited the niobium coating on M1 copper, MAGT-0.05 copper alloy, and MAGT-0.2 copper alloy, and measured the mutual diffusion coefficient of niobium. The dynamic process of preparing surface composites by molten salt electrochemical method includes three steps: mass transfer of particles in molten salt, reduction of ions, and solid diffusion of atoms in the matrix. The studies on the mass transfer process and electrochemical reduction process of particles in molten salt are more compared to the studies on solid diffusion process of matrix. The solid-state diffusion process of

---

* **Corresponding author: Yungang Li,** Key Laboratory of Ministry of Education for Modern Metallurgy Technology, College of Metallurgy and Energy, North China University of Science and Technology, Tangshan 063009, China, e-mail: liyungang59322@163.com
Shixian Zhang, Xiaoping Zhao: Department of Materials Engineering, Hebei Vocational University of Industry and Technology, Shijiazhuang 050091, China
Kai Hu: CAS Key Laboratory of Green Process and Engineering, Institute of Process Engineering, Chinese Academy of Sciences, Beijing 100190, China
Jinglong Liang: Key Laboratory of Ministry of Education for Modern Metallurgy Technology, College of Metallurgy and Energy, North China University of Science and Technology, Tangshan 063009, China

atoms in the matrix should also be considered to comprehensively study the whole dynamic process.

The drawbacks of easy oxidation and corrosion of low-carbon steel severely limit its application in certain special requirement areas. At the same time, the lack of chromium and nickel resources and high prices limit the production and application range of stainless steel. Therefore, preparing a Cr–Ni alloy/low-carbon steel surface composite material can combine the excellent properties of the two materials to make up for the shortcomings, and has important theoretical significance and practical value for saving resources and expanding the range of material use. In this study, the Cr–Ni alloy/low-carbon steel surface composites were successfully prepared by electrochemical deposition method in NaCl–KCl–NaF–Cr_2O_3–NiO molten salt system. It not only improved the corrosion resistance of low-carbon steel substrate, but also greatly reduced the preparation cost of materials. The diffusion coefficients of chromium and nickel atoms in low-carbon steel were calculated through experiments and dynamic calculations, and the overall diffusion dynamic behavior in the preparation process was discussed. The research results can provide ideas for improving the efficiency of molten salt electrodeposition.

2 Experimental method

2.1 Materials and treatment

The raw materials selected for molten salt system include analytically pure NaCl, KCl, NaF, Cr_2O_3, and NiO. According to $X_{NaCl}:X_{KCl}:X_{NaF} = 2:2:1$ molar ratio of molten salt components, and 2% molar content of Cr_2O_3 and NiO, 200 g analytically pure reagents were weighed to ensure sufficient chromium and nickel sources in the process of molten salt electrolytic deposition.

First, grind the used initial reagents into powder, then place the reagents in a vacuum drying oven, dry it at 493 K for 720 min to remove the crystal water in the reagents. Second, put the cooled reagents into a 50 ml high-purity graphite crucible, and cover it for sealing. Finally, put the crucible into a closed well type resistance furnace, and pass $100\ \text{ml}\cdot\text{min}^{-1}$ argon for protection. When the temperature reaches 1,073 K, keep the heat for 7 h to saturate the molten salt [12,13].

2.2 Electrochemical detection

The Zahner electrochemical workstation (IM6eX, Germany) and three electrode detection systems were used to measure the parameters of relevant electrochemical reactions in the molten salt system (Figure 1).

Because the common reference electrode cannot work in high temperature molten salt, we chose the platinum electrode with good reversibility, high exchange current density, stable potential, and good reproducibility as the reference electrode. The working electrode, reference electrode, and counter electrode were all made of 99.99% platinum. Keep the distance between the three electrodes at 10 mm during the detection. First, an alumina tube having an inner diameter of 0.6 mm was used as the sleeve to protect the platinum wire with a diameter of 0.5 mm. Two platinum wires of length 1 cm at the upper and lower ends of the corundum tube were used as the reference electrode and working electrode, and the other platinum wire is connected with the platinum sheet as the counter electrode. Second, the platinum sheet was polished slightly with 5,000 mesh sandpaper, washed with 5% dilute hydrochloric acid for 1 min, put into anhydrous ethanol, and shaken with an ultrasonic cleaner for 5 min. Third, the three electrodes were inserted into the molten salt, and connected to the electrochemical workstation to conduct electrochemical measurement in the NaCl–KCl–NaF–Cr_2O_3–NiO molten salt.

Before the formal measurement, pre-electrolysis was performed for 2 h at a constant voltage of 2 V to remove

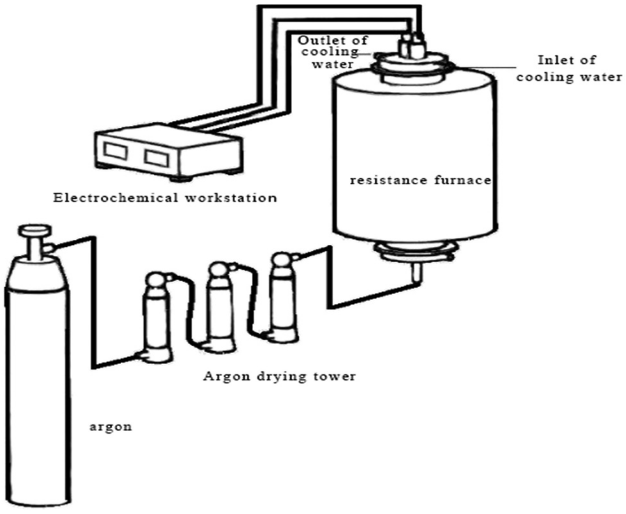

Figure 1: Schematic diagram of electrochemical detection system.

Table 1: Composition of low-carbon steel plate

Element	C	Si	Mn	P	S	Fe
Content (wt%)	0.10	0.10	0.3	0.02	0.02	Remaining amount

residual water, oxide anions, and other compounds. And then the chronoamperometry curves of the molten salt were measured in the potential range of −0.33 to −0.98 V.

2.3 Electrodeposition

Two electrode system was used to carry out electrodeposition experiment. The anode material is high-purity graphite plate. The cathode material is Q-195 low-carbon steel plate, and its specific composition is shown in Table 1. Before the experiment, 20 mm × 20 mm × 3 mm low-carbon steel plate was polished with silicon carbide sandpaper (320, 800, 1,000, 1,500, and 2,000 mesh), and then soaked in 5% NaOH hydrothermal solution for 5 min to remove grease. The pickling was soaked in 5% hydrochloric acid solution for 1 min, then rinsed in an ultrasonic cleaner for 5 min with ethanol, and blown dry with a blower to remove surface impurities. The 20 mm × 50 mm × 3 mm high-purity graphite anode was cleaned by ultrasonic cleaner containing 10% hydrochloric acid solution for 5 min, rinsed with deionized water, and blown dry.

The processed cathode and anode electrodes were inserted into the molten salt, and the electroplating power (SMD-P, China) was switched on to carry out the molten salt electrodeposition experiment. The specific electrodeposition conditions are shown in Table 2.

2.4 Analysis and detection

The contents of chromium and nickel in the surface composites of low-carbon steel along the diffusion layer were detected by GDA750 glow discharge spectrometer.

3 Results and discussion

3.1 Analysis of diffusion dynamics results

3.1.1 Kinetic analysis of ion diffusion in molten salt

Figure 2 shows the chronoamperometric curve measured by applying different electrode potentials to the molten salt system. The chronoamperometric curves measured at each electrode potential are typical chronoamperometric curves, which conform to the characteristics that ion diffusion in solution is the control link [14]. The reduction process of chromium and nickel ions on the cathode is shown on the chronoamperometric curve. With the gradual increase in potential, there are three steps in the curve. The first step (−0.39 to −0.41 V) represents the process of Ni^{2+} being reduced to metal Ni, the second step (−0.60 to −0.63 V) represents the process of Cr^{3+} being reduced to Cr^{2+}, and the third step (−0.95 to −0.98 V) represents the process of Cr^{2+} being reduced to metal Cr. At the beginning of the experiment, the circuit is in an open circuit state with the potential of 0. When the constant potential is applied, the double electric layer on the electrode surface charges rapidly, generating current on the cathode, and then decreases rapidly. At the same time, chromium and nickel ions begin to reduce on the cathode surface. With the extension of time, the concentration of chromium and nickel ions near the cathode surface decreases continuously, leading to concentration polarization which reduce the current to a steady state slowly [15].

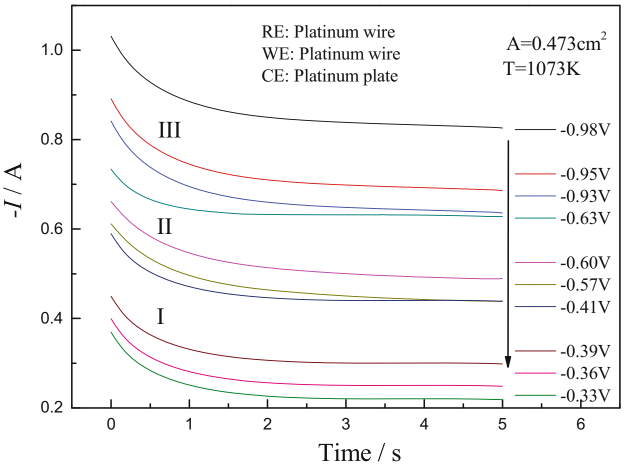

Figure 2: Chronoamperometric curves of cathodes with different potentials in NaCl–KCl–NaF–Cr_2O_3–NiO molten salt at 1,073 K.

3.1.2 Diffusion dynamics of reduced atoms on the surface of Cr–Ni alloy/low-carbon steel surface composite

Figure 3 shows the metallographic photo, SEM photo, energy spectrum analysis results, and XRD pattern of

Table 2: Parameter of electrodeposition process in molten salt

Electrode spacing (mm)	Bidirectional pulse current	Current density (mA·cm^{-2})	Temperature (K)	Time (min)
20	1,000 ms, $i_{positive}$:$i_{reverse}$ = 6:1, $t_{positive}$:$t_{reverse}$ = 3:1	300	1,073	180

the Cr–Ni alloy/low-carbon steel deposited in the NaCl–KCl–NaF–Cr_2O_3–NiO molten salt for 180 min at 1,073 K. It can be seen from the metallographic photos and scanning electron microscope photos that a deposition diffusion layer is formed on the surface of the substrate. The iron content is 70.09 wt%, chromium content is 6.14 wt%, and nickel content is 23.77 wt%. It can be seen from the XRD pattern that the diffraction peak of the product is consistent with the standard spectrum of Ni–Cr–Fe alloy (35–1,375). It illustrates that the Cr–Ni alloy and low-carbon steel are mutually diffused under the action of high temperature during electrodeposition to form the Cr–Ni alloy/low-carbon steel surface composite.

Figure 4 shows the relationship between the element content and the depth of the sample. It can be seen that the content of chromium and nickel decreases with the increase in the section depth of the sample, and the content of iron increases with the increase in the section depth of the sample. It shows that chromium, nickel, and iron inter diffused on the surface of low-carbon steel, and a gradient layer with a certain thickness is formed. The Cr–Ni alloy/low-carbon steel surface composite was prepared by means of molten salt electrodeposition and solid-state diffusion.

In the actual diffusion process, the diffusion coefficient of elements in the matrix changes with the concentration of diffusing elements.

In order to obtain the atomic diffusion law of Cr–Ni alloy/low-carbon steel surface composite prepared by molten salt co-deposition process, the diffusion

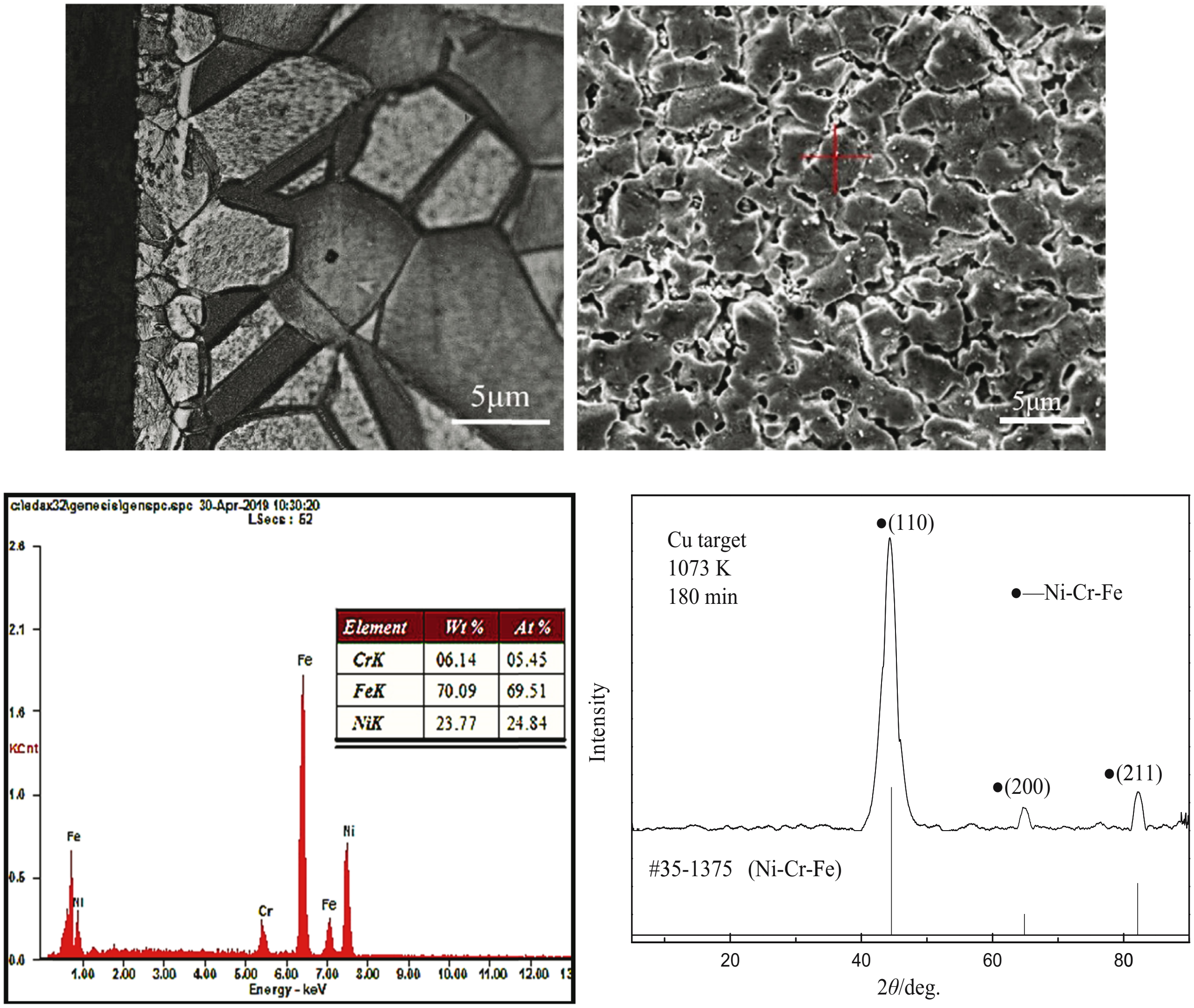

Element	Wt %	At %
CrK	06.14	05.45
FeK	70.09	69.51
NiK	23.77	24.84

Figure 3: Cross section metallographic photograph, surface SEM image, EDS test, and XRD pattern of Cr–Ni alloy sample co-electrodeposited in molten salts under different conditions (1,073 K, 300 mA·cm^{-2}, 180 min).

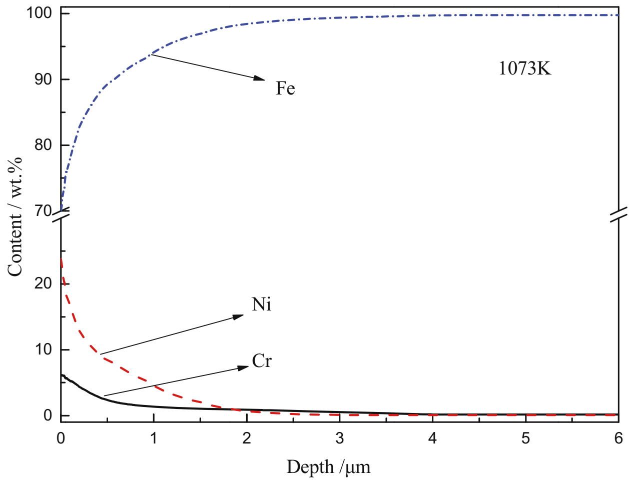

Figure 4: Relationship between element content and section depth of co-deposition sample in molten salt at 1,073 K.

coefficients at different volume concentrations are calculated by Fick's second law, Arrhenius law [16], and Den Broeder formula [17] (formula (1)) under fixed temperature conditions. And the average diffusion coefficient of the atom is obtained by fitting and averaging the obtained diffusion coefficient curve within the measured volume concentration range to reflect the general law of diffusion coefficient of diffusing atoms at a specific temperature.

$$D_{C_B^*} = \frac{1}{2t\left(\frac{\partial C_B}{\partial x}\right)_{x^*}}\left[(1-y_C^*)\int_{-\infty}^{x^*}(C_B^*-C_{B_1})\mathrm{d}x + y_C^*\int_{x^*}^{+\infty}(C_{B_2}-C_B^*)\mathrm{d}x\right]. \tag{1}$$

Taking the surface as zero in the percentage content curves of chromium and nickel, nine groups of percentage contents and corresponding depths were obtained, respectively, in the range of nickel 1–21% (step length 2.5%) and chromium 0.5–6.5% (step length 0.75%). The data of different element volume concentrations and matrix depth were fitted by Boltzmann function, and the fitting equations $C_{\mathrm{Cr}} = f(x)$ and $C_{\mathrm{Ni}} = f(x)$ of chromium and nickel diffusion were obtained, respectively.

According to Den Broeder formula, Matlab software is used to calculate the mathematical expression of the diffusion fitting equation $\int_{x^*}^{+\infty}(C_{B_2}-C_{C_B^*})\mathrm{d}x$, $\int_{-\infty}^{x^*}(C_{C_B^*}-C_{B_1})\mathrm{d}x$, and $(\partial C_B/\partial x)_{x^*}$ of chromium and nickel atoms on the surface of low-carbon steel at 1,073 K. Finally, the diffusion coefficients of chromium and nickel atoms at different depths and concentrations are obtained. Figure 5 shows the variation in diffusion coefficient of chromium and nickel atoms with depth and percentage content.

The law in Figure 5 was solved by integral method, and the average diffusion coefficient of chromium and nickel in the surface of low-carbon steel at 1,073 K was obtained, as shown in Table 3.

$$\bar{D} = \frac{\int_{C_1}^{C_2} D(C)\mathrm{d}C}{C_2 - C_1}. \tag{2}$$

3.2 Discussion on diffusion process

The process of co-deposition of Cr–Ni alloy/low-carbon steel surface composites in molten salt is determined by the combined effect of active particles mass transfer,

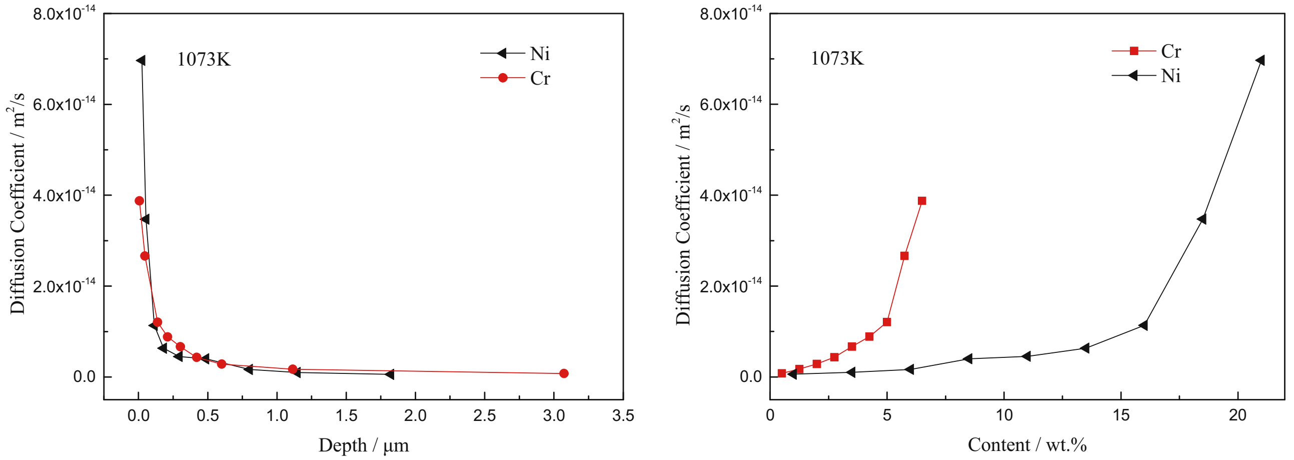

Figure 5: Relationship between Cr and Ni diffusion coefficients and section depth and concentration of samples co-deposited in molten salt (1,073 K, 180 min).

Table 3: Average diffusion coefficients of Cr and Ni of samples co-deposited in molten salt (1,073 K, 180 min)

Element	Fitting curve $D = f(C)$	R	Average diffusion coefficient ($m^2 \cdot s^{-1}$)
Cr	$D = \exp(-29.94 - 17.55/(C + 3.53))$	0.99553	1.16×10^{-14}
Ni	$D = \exp(-36.20 + 0.28\,C - 0.01C^2)$	0.99352	1.44×10^{-14}

electrochemical reduction, and solid-state diffusion. The specific process is shown in Figure 6. A large number of active particles in molten salt undergo irregular Brownian motion in molten salt. After the unidirectional current is applied to the system, the active particles move directionally under the action of the electric field, and concentrate near the cathode surface to form an electric double layer [18–20]. Chromium and nickel ions close to the cathode get electrons to be reduced to atoms, and are adsorbed on the cathode surface to form another concentration gradient with the cathode material. Chromium, nickel atoms and cathode will mutually diffuse in solid-state at high temperature, and finally Cr–Ni alloy/low-carbon steel surface composite will be obtained.

The typical chronoamperometric curves conform to the characteristics that ion diffusion in solution is the control link. This shows that the mass transfer rate of active particles is the limiting link in the whole preparation process, which affects the preparation rate of materials. Under the action of the directional electric field, the chromium and nickel active particles are concentrated on the cathode surface. The high concentration of active particles is helpful to improve the electrochemical reduction reaction speed. However, due to the high electrochemical reduction speed, the active ion concentration in the electric double layer cannot be rapidly supplemented, which reduces the speed of the whole preparation process.

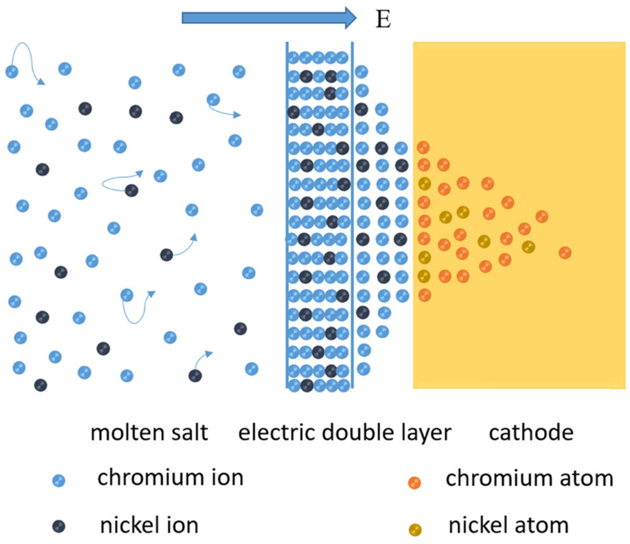

Figure 6: Dynamic diagram of electrodeposition process in molten salt.

4 Conclusion

The Cr–Ni alloy/low-carbon steel surface composites were prepared by molten salt co-deposition in NaCl, KCl, NaF, Cr_2O_3, and NiO melt salt system, and the kinetics of the preparation process was systematically studied. The results show that a certain thickness of alloy gradient layer is prepared on the surface of low-carbon steel under the combined action of the mass transfer of chromium and nickel active particles in molten salt, electrochemical reduction, and high-temperature solid diffusion. The chromium and nickel ions are simultaneously reduced on the cathode surface through two and one steps, respectively. According to the detection data of the deposition layer, the average diffusion coefficients of chromium and nickel atoms in the surface composite are calculated to be 1.16×10^{-14} and 1.44×10^{-14} $m^2 \cdot s^{-1}$. Affected by the mass transfer rate, the concentration of ions in the electric double layer near the cathode cannot be rapidly supplemented, thus reducing the speed of the entire preparation process.

Funding information: The study is financially supported by the National Natural Science Foundation of China (Project No. 51974129), and the Hebei Province “three three three talent project” Funding (Project No. A202101030).

Author contributions: Shixian Zhang: conceptualization, writing – review and editing, methodology, and formal analysis; Kai Hu: original draft and methodology; Xiaoping Zhao: original draft, software, and methodology; Jinglong Liang: methodology, formal analysis, and validation; Yungang Li: conceptualization, validation, and funding acquisition. All authors have read and agreed to the published version of the manuscript.

Conflict of interest: Authors state no conflict of interest.

Data availability statement: Data sharing is not applicable for this article.

References

[1] Sun, N., Y. Zhang, F. Jiang, S. Lang, and M. Xia. Preparation of tungsten coatings on graphite by electro-deposition via Na_2WO_4-WO_3 molten salt system. *Fusion Engineering and Design*, Vol. 11, 2014, pp. 2529–2533.
[2] Dubrovskiy, A., O. Makarova, and S. Kuznetsov. Effect of the molybdenum substrate shape on Mo_2C coating electrodeposition. *Coatings*, Vol. 8, 2018, pp. 442–453.
[3] Yasuda, K., K. Saeki, T. Kato, R. Hagiwara, and T. Nohira. Silicon electrodeposition in a water-soluble KF-KCl molten salt: effects of temperature and current density. *Journal of the Electrochemical Society*, Vol. 16, 2018, pp. D825–D831.
[4] Zhang, H. *Research on electrochemical reduction of Ce(III) in chloride molten salt and alloy preparation mechanism*, Jiangxi University of Science and Technology, Jiangxi, Chian, 2022.
[5] Huang, H., B. Yu, Q. Yan, G. Chen, Q. Zhang, and Y. Liu. Study on electrochemical behavior of Y(III) in Molten YF3-LiF. *Rare Metals and Cemented Carbides*, Vol. 49, 2021, pp. 5–8 + 23.
[6] Wang, Q., L. Zhang, L. Zhai, J. Li, and J. Zhang. In-situ synthesis of silicide coatings on molybdenum substrates by electrodeposition in chloride-fluoride molten salts. *International Journal of Refractory Metals and Hard Materials*, Vol. 82, 2019, pp. 340–348.
[7] Huang, Y., S. Bai, H. Zhang, and Y. Ye. Growth mechanism and mechanical property of laminar iridium coating by electrodeposition. *International Journal of Refractory Metals and Hard Materials*, Vol. 50, 2015, pp. 204–209.
[8] Huang, Y., S. Bai, H. Zhang, and Y. Ye. Oxidation of iridium coating on rhenium coated graphite at elevated temperature in stagnated air. *Applied Surface Science*, Vol. 328, 2015, pp. 436–443.
[9] Huang, Y., S. Bai, H. Zhang, Y. Ye, and L. Zhu. Oxidation of iridium coatings on rhenium substrates at ultrahigh temperature in stagnant air: Its failure mechanism and life model. *Surface and Coatings Technology*, Vol. 288, 2016, pp. 52–61.
[10] Huang, Y., S. Bai, H. Zhang, and Y. Ye. Sealing of cracks in the rhenium coating on C/C composites by alloying with cobalt. *Surface and Coatings Technology*, Vol. 261, 2015, pp. 404–410.
[11] Kuznetsov, S. Electrodeposition of niobium coatings on long conductors from a copper alloy. *Journal of the Electrochemical Society*, Vol. 116, 2019, pp. D694–D699.
[12] Li, M., X. Meng, Y. Liu, H. Zhang, X. Li, and Y. Li. Solubility and dissolution mechanism of NiO in NaCl-KCl-NaF molten salt system. *Nonferrous Metals Engineering*, Vol. 3, 2019, pp. 57–61.
[13] Zhang, H., S. Zhang, H. Li, T. Ma, Y. Cao, X. Li, et al. Study on solubility of Cr_2O_3 in NaCl-KCl-NaF molten salt system. *Inorganic Chemicals Industry*, Vol. 2, 2019, pp. 22–25.
[14] Liu, M., Y. Xing, J. Wang, D. Wang, L. Huang, X. Wu, et al. Besides the capacitive and diffusion control: Inner-surface controlled bismuth based electrode facilitating potassium-ion energy storage. *Advanced Functional Materials*, Vol. 31, 2021, id. 2101868.
[15] Zhang, S., Y. Li, K. Hu, X. Zhao, H. Li, and J. Liang. Preparation of Cr–Ni alloy by electrochemical codeposition in a NaCl-KCl-NaF-Cr_2O_3-NiO molten salt. *International Journal of Electrochemical Science*, Vol. 13, 2018, pp. 8030–8041.
[16] Dong, Y., Y. Wang, and F. Zhang. *Inorganic and analytical chemistry*, 3rd ed., Science Press, Beijing, China, 2011, pp. 59–60. ISBN 9787030300652.
[17] Den, B. F. A general simplification and improvement of the Matano-Boltzmann method in the determination of the interdiffusion coefficients in binary systems. *Scripta Metallurgica*, Vol. 3, 1969, pp. 321–325.
[18] Li, H., J. Liang, H. Yan, Y. Li, and L. Wang. Preparation of Gradient Materials with Molten Salts Electrodeposition. *Crystals*, Vol. 11, 2021, id. 590.
[19] Bard, A. J. and L. R. Faulkner. *Electrochemical methods: Fundamentals and applications*, Wiley, New York, USA, 1983, pp. 103–110. ISBN 0-471-05542-5.
[20] Yang, D., S. Jiang, Y. Liu, T. Yin, M. Li, L. Wang, et al. Electrodeposition mechanism of La^{3+} on Al, Ga and Al-Ga alloy cathodes in LiCl-KCl eutectic salt. *Journal of the Electrochemical Society*, Vol. 168, 2021, id. 062511.